

Mach number and plasma beta dependence of the ion temperature perpendicular to the external magnetic field in the transition region of perpendicular collisionless shocks

Ryo Yamazaki,^{1, a)} Ayato Shinoda,¹ Takayuki Umeda,^{2, b)} and Shuichi Matsukiyo^{3, c)}

¹⁾*Department of Physics and Mathematics, Aoyama Gakuin University, Sagamihara 252-5258, JAPAN.*

²⁾*Institute for Space-Earth Environmental Research, Nagoya University, Nagoya 464-8601, JAPAN*

³⁾*Department of Earth System Science and Technology, Kyushu University, Kasuga 816-8580, JAPAN*

Ion temperature anisotropy is a common feature for (quasi-)perpendicular collisionless shocks. By using two-dimensional full particle simulations, it is shown, that the ion temperature component perpendicular to the shock magnetic field at the shock foot region is proportional to the square of the Alfvén Mach number divided by the plasma beta. This result is also explained by a simple analytical argument, in which the reflected ions get energy from upstream plasma flow. By comparing our analytic and numerical results, it is also confirmed that the fraction of the reflected ions hardly depends on the plasma beta and the Alfvén Mach number when the square of the Alfvén Mach number divided by the plasma beta is larger than about 20.

In various kinds of solar-terrestrial, astrophysical and laboratory plasmas, ubiquitous is the collisionless shock, at which the upstream kinetic energy of the supersonic plasma flow dissipates into downstream energy of thermal ions and electrons, waves (turbulence), and nonthermal particles.^{1,2} Despite various kinds of studies, detailed processes of the shock dissipation remain to be clarified. For example, we do not fully understand how energies are partitioned between downstream thermal electrons and ions, although the total pressure of them can be simply predicted by the fluid Rankine-Hugoniot relation.

For supercritical (quasi-)perpendicular shocks, a fraction of incoming ions can be specularly reflected toward the upstream region but gyrates back to the shock front.³⁻¹⁰ Such reflected-gyrating ions can gain energy from the motional electric field of the upstream plasma flow and contribute to the increase of the ion temperature component perpendicular to the local magnetic field. Consequently, a large temperature anisotropy arises at the shock foot, exciting waves through the ion temperature anisotropy instability, which is responsible for the shock ripples.^{11,12} Electron preheating at the foot also takes place under some conditions.^{3,13,14} The ripple further dissipates ions, increasing ion parallel temperature, and even electron acceleration occurs.¹⁵ In the downstream region, the ion distribution is no longer non-gyropropic and its structures are smoothed out by collisionless gyrophase mixing, resulting in the downstream ion heating.¹⁶⁻²¹ In order to understand such a multi-step dissipation process across the shock front, it is important to estimate the initial ion temperature component perpendicular to the shock magnetic field at the foot region. In the present study, using the two-dimensional full

particle simulation of low-Mach-number, perpendicular, rippled and collisionless shocks, we study the ion perpendicular temperature at the shock foot region. We show, for the first time, that it is proportional to the square of the Alfvén Mach number divided by the plasma beta, or the square of the sonic Mach number, which is consistent with the analytical scaling relation.⁵

We perform two-dimensional (2D) simulations of perpendicular ($\theta_{B_n} = 90^\circ$) collisionless shocks by using a standard particle-in-cell code.²² As in our previous works,^{15,23,24} the shock is excited by the “relaxation” between a supersonic and a subsonic plasma flows moving in the same direction. The initial state consists of the two regions separated by a discontinuity. Both regions have spatially uniform distributions of electrons and ions with different bulk flow velocities, temperatures, and densities, and they have uniform perpendicular magnetic field with different strength. The simulation domain is taken in the x - y plane and an in-plane shock magnetic field (B_{y0}) is assumed. We apply a uniform external electric field $E_{z0} = u_{x1}B_{y01}/c$ ($= u_{x2}B_{y02}/c$) in both upstream and downstream regions, so that both electrons and ions drift along the x axis. Here, u_x is the bulk flow velocity, and subscripts “1” and “2” denote “upstream” and “downstream”, respectively. At the left (right) boundary of the simulation domain in the x direction, we inject plasmas with the same quantities as those in the initial upstream (downstream) region. We use absorbing boundaries to suppress non-physical reflection of electromagnetic waves at both ends of the simulation domain in the x direction,²⁵ while the periodic boundaries are imposed in the y direction.

In the present study, we present results of six simulations runs (A, B, C, D, E and F) with different upstream conditions. We summarize in TABLE I the upstream plasma parameters, such as the bulk flow velocity u_{x1} , the ratio of the electron plasma frequency to the electron cyclotron frequency $\omega_{pe1}/\omega_{ce1}$. For all runs,

^{a)}Email:ryo@phys.aoyama.ac.jp.

^{b)}Email:umeda@isee.nagoya-u.ac.jp

^{c)}Email:matsukiyo@esst.kyushu-u.ac.jp

we fix ion-to-electron mass ratio $m_i/m_e = 256$, and set $v_{te1}/c = 0.1$, where v_{te1} and c are the electron thermal velocity upstream and the speed of light, respectively. In the following, subscripts “i” and “e” represent “ion” and “electron”, respectively. Then, we obtain the plasma beta $\beta_1 = 2(v_{te1}/c)^2(\omega_{pe1}/\omega_{ce1})^2$, and $u_{x1}/V_{A1} = (m_i/m_e)^{1/2}(v_{te1}/c)(\omega_{pe1}/\omega_{ce1})(u_{x1}/v_{te1})$, where V_{A1} is the upstream Alfvén velocity, respectively. It is assumed that the electrons and ions have the same plasma beta, $\beta_{e1} = \beta_{i1} = \beta_1$, and the same isotropic temperature, $T_{e1} = T_{i1}$. Here, temperatures and thermal velocities are related as $T_{e1} = m_e v_{te1}^2$ and $T_{i1} = m_i v_{ti1}^2$. For given upstream frequencies ω_{pe1} and ω_{ce1} , the initial upstream number density $n_1 \equiv m_e \omega_{pe1}^2 / 4\pi e^2$ and the initial magnetic field strength $B_{y01} = m_e \omega_{ce1} / e$ are derived. Then, the initial downstream parameters are determined by solving the shock jump conditions (Rankine-Hugoniot conditions) for a magnetized two-fluid isotropic plasma consisting of electrons and ions,²⁶ assuming $T_{i2}/T_{e2} = 8.0$.

The grid spacing and the time step of the present simulation runs are set to be $\Delta x = \Delta y \equiv \Delta = \lambda_{De1}$ and $c\Delta t/\Delta = 0.5$, where λ_{De} is the electron Debye length. The total size of the simulation domain is $32l_{i1} \times 6l_{i1}$, where $l_{i1} = c/\omega_{pi1} = (m_i/m_e)^{1/2}(c/v_{te1})\lambda_{De1}$ is the ion inertial length of the upstream plasma. We used 25 pairs of electrons and ions per cell in the upstream region and 64 pairs of electrons and ions per cell in the downstream region, respectively, at the initial state.

In the following, the ion temperature component perpendicular to the shock magnetic field is approximated by the arithmetic mean of ion temperatures in x and z directions, that is, $T_{i\perp} = (T_x + T_z)/2$. In Fig. 1, we show spatiotemporal evolution of B_y (left panel) and $T_{i\perp}$ (right panel) for Run D. Here both of them are averaged over the y direction. The initial unphysical disturbance disappears and the growth of the shock ripples ceases until $\omega_{ci1}t = 7.0$, after which the shock structure seems to be in the quasi-steady state. Unlike one-dimensional simulation, quasi-periodic reformation seems unclear, although we can still see the front oscillation. Hence, in the following, we analyze the data after $\omega_{ci1}t = 7.0$ for all runs.

As shown in FIG. 1, the shock front moves leftward in our simulation frame. Using spatiotemporal diagram of B_y , we measure the shock velocity v_{sh} , and obtain the Alfvén Mach number, $M_A = (u_{x1} - v_{sh})/V_{A1}$, in the shock-rest frame. The results for all six runs are shown in TABLE I.

We extract the representative value of $T_{i\perp}$ in the transition layer for each run as follows. First, we make a snapshot of $T_{i\perp}$ which is averaged over y direction, and find its maximum value, $T_{i\perp}^{\max}$, for each time step. As shown in FIG. 2, one can find that $T_{i\perp}$ has a maximum at the foot region. This fact is also true in arbitrary epoch. The value of $T_{i\perp}^{\max}$ changes with time. Then, the time mean of $T_{i\perp}^{\max}$ for $7 \leq \omega_{ci1}t \leq 12$ is obtained. For example, we obtain the average value $T_{i\perp}^{\max}/T_{i1} = 101$ and

the maximum and minimum values are 123 and 86.5, respectively. In the same way, the average, maximum, and minimum values of $T_{i\perp}^{\max}$ are obtained for other runs. The results are summarized in TABLE I. In FIG. 3, $T_{i\perp}^{\max}/T_{i1}$ is shown as a function of M_A^2/β_1 . The simulation results seem to lie on the line, $T_{i\perp}^{\max}/T_{i1} \approx 0.5 \times M_A^2/\beta_1$.

In the following, we derive a simple analytical formula to have the ion perpendicular temperature at the shock foot. Although similar formulae have been already derived,⁵⁻⁷ our final equation, Eq. (11), is in an excellent agreement with our simulation results. In our simulation frame, shock front moves at a velocity v_{sh} , and upstream and downstream bulk velocities are typically u_{x1} and u_{x2} , respectively. The incoming ions are adiabatically heated at the shock foot. They have the perpendicular temperature, $[C^{\gamma-1}/(\gamma-1)]m_i v_{ti1}^2$, where $C \sim (n_{i,f}/n_{i1})$ is a compression factor, and γ and $n_{i,f}$ are the adiabatic index ($\gamma = 2$ in our case) and the typical value of the density at the foot, respectively. Since they are also decelerated and due to the mass flux conservation, their bulk velocity becomes $u_{(\text{in})} \approx v'_{sh}/C$ measured in the rest frame of the shock front, where $v'_{sh} = u_{x1} - v_{sh} = M_A V_{A1}$. Next, a part of them are reflected. The bulk velocity of the reflected ions is $u_{(\text{ref})} \approx -v'_{sh}/C$ in the shock rest frame.⁴ Hence, we have the velocity difference between the incoming and the reflected ions,

$$\Delta u \approx u_{(\text{in})} - u_{(\text{ref})} \approx \frac{2v'_{sh}}{C} \quad , \quad (1)$$

at the shock foot. A large fraction of energy (per ion), $(m_i/2)|\Delta u|^2$, is consumed for increasing the ion perpendicular temperature.

Here, we consider a simple analytical model to estimate $T_{i\perp}$ at the foot region. The ion distribution function there is written as

$$f_{\text{tot}}(v_x) = f_{(\text{in})}(v_x) + f_{(\text{ref})}(v_x) \quad , \quad (2)$$

where the first and the second terms in r.h.s. describe the incoming and reflected components, respectively, and they have the number density $N_{(\text{k})}$, bulk velocity $u_{(\text{k})}$, and temperature $T_{(\text{k})}$ as

$$N_{(\text{k})} = \int f_{(\text{k})} dv_x \quad , \quad (3)$$

$$u_{(\text{k})} = \frac{1}{N_{(\text{k})}} \int v_x f_{(\text{k})} dv_x \quad , \quad (4)$$

$$T_{(\text{k})} = \frac{m_i}{N_{(\text{k})}} \int (v_x - u_{(\text{k})})^2 f_{(\text{k})} dv_x \quad , \quad (5)$$

respectively. A subscript (k) = (in), (ref) denotes each component. Then, it is natural to approximate $T_{i\perp}$ as

$$T_{i\perp} \approx T_x = \frac{m_i}{N_{\text{tot}}} \int (v_x - \bar{u})^2 f_{\text{tot}} dv_x \quad , \quad (6)$$

where N_{tot} and \bar{u} are given by

$$N_{\text{tot}} = \int f_{\text{tot}} dv_x = N_{(\text{in})} + N_{(\text{ref})} \quad , \quad (7)$$

$$\bar{u} = \frac{1}{N_{\text{tot}}} \int v_x f_{\text{tot}} dv_x \quad , \quad (8)$$

respectively. When we introduce the fraction of the reflected ions as $r = N_{(\text{ref})}/N_{\text{tot}}$, then we get

$$T_{i\perp} = T_{(\text{in})} + r(T_{(\text{ref})} - T_{(\text{in})}) + m_i[(1-r)u_{(\text{in})}^2 + ru_{(\text{ref})}^2 - \bar{u}^2] \quad (9)$$

and $\bar{u} = (1-r)u_{(\text{in})} + ru_{(\text{ref})}$. Assuming $T_{(\text{in})} = T_{(\text{ref})}$ as in one of our previous simulation study²⁷ and eliminating \bar{u} , we can rewrite Eq. (9) as

$$T_{i\perp} = T_{(\text{in})} + r(1-r)m_i(u_{(\text{in})} - u_{(\text{ref})})^2 \quad (10)$$

Using Eq. (1) together with $T_{(\text{in})} = CT_{i1}$ and $m_iv'_{sh}{}^2/T_{i1} = 2M_A^2/\beta_1$, we finally obtain

$$\frac{T_{i\perp}}{T_{i1}} = C + \frac{8r(1-r)}{C^2} \frac{M_A^2}{\beta_1} \quad (11)$$

The first term in r.h.s of Eq. (11) is important for the case of low M_A^2/β_1 only. The compression factor C is slightly larger than unity for such shocks. For large M_A^2/β_1 , the second term dominates r.h.s of Eq. (11), so that we can explain our numerical result, $T_{i\perp}^{\text{max}}/T_{i1} \propto M_A^2/\beta_1$, shown in FIG. 3, if the factor $8r(1-r)/C^2$ in Eq. (11) hardly depends on M_A^2/β_1 . The fraction of the reflected ions is typically $r \approx 0.3$ and varies from 0.2 to 0.4 during non-stationary processes at the shock front. On the other hand, the value of C is less variable and ranges between 1.0 and 1.1. Then, one can see $8r(1-r)/C^2 = 1.1 - 1.9$. This is a factor of a few larger than estimated from FIG. 3. Indeed, our analytical formula, Eq. (11), gives the upper bound of $T_{i\perp}$, because the free energy $m_i(\Delta u)^2$ goes not only to $T_{i\perp}$ but also to the thermal energy of reflected ions and waves excited in the shock transition layer.²⁸ In practice, one can see that $T_{i\perp}$ becomes larger if $T_{(\text{ref})} > T_{(\text{in})}$ [see Eq. (9)]. Note that the fraction of the reflected ions, r , estimated in the previous analytical works^{4,8,29} is slightly smaller than that obtained from our simulations.

In the present study, we focus on $T_{i\perp}$ only. On the other hand, the parallel component of ion temperature ($T_{i\parallel} \approx T_y$) is much smaller at the foot region. Therefore, the total ion temperature, $T_i = (T_x + T_y + T_z)/3 = (2T_{i\perp} + T_{i\parallel})/3$, is approximated as $T_i \approx (2/3)T_{i\perp}$.

Using two-dimensional full particle simulations, we have shown that the ion perpendicular temperature at the foot of the supercritical perpendicular collisionless shocks is proportional to M_A^2/β_1 , or the square of the sonic Mach number. This fact will give us a simple estimate of the energy partition between downstream thermal ions and electrons, although further study is necessary. The ion heating at the foot region of (quasi-)perpendicular shocks has been extensively investigated by many authors, using mainly spacecraft observations,^{5,9} (semi-)analytical studies,^{4,5} and one-dimensional hybrid simulations.⁷ In this paper, we have extended such studies by using two-dimensional full particle simulations which can better capture various kinetic effects including wave excitations and plasma heating in the direction tangential to the shock front. More

specifically, we have demonstrated in this paper that our analytical scaling relation Eq. (11) is in excellent agreement with two-dimensional full particle simulations of rippled shocks. This result also indicates that the dependence of fraction of ion reflection on the plasma beta and the Alfvén Mach number is small when M_A^2/β is larger than about 20, which is consistent with our simulation results.

ACKNOWLEDGMENTS

The authors would like to thank Yutaka Ohira for helpful comments. The computer simulations were performed on the CIDAS supercomputer system at the Institute for Space-Earth Environmental Research in Nagoya University under the joint research program. This work was partly supported by JSPS KAKENHI Grants: 15K05088, 18H01232 (RY), 2628704, 19H01868 (TU).

- ¹A. Balogh and R. A. Treumann, *Physics of Collisionless Shocks* (Springer, New York, 2013)
- ²D. Burgess and M. Scholer, *Collisionless Shocks in Space Plasmas* (Cambridge University Press, Cambridge, 2015)
- ³L. C. Woods, *Plasma Phys.* **13**, 289 (1971).
- ⁴M. M. Leroy, *Phys. Fluids.* **26**, 2742 (1983).
- ⁵N. Scopke, G. Paschmann, S. J. Bame, and J. T. Gosling, *J. Geophys. Res.* **88**, 6121 (1983).
- ⁶J. T. Gosling and A. E. Robson, In *collisionless shocks in the heliosphere: Reviews of current research*, **35**, 141. Washington, DC: American Geophysical Union (1985).
- ⁷D. Burgess, W. P. Wilkinson, and S. J. Schwartz, *J. Geophys. Res.* **94**, 8783 (1989).
- ⁸W. P. Wilkinson and S. J. Schwartz, *Planet Space Sci.* **38**, 419 (1990).
- ⁹N. Scopke, G. Paschmann, A. L. Brinca, C. W. Carlson, and H. Lüth, *J. Geophys. Res.* **95**, 6337 (1990).
- ¹⁰B. Lembège and P. Savoini, *Phys. Fluids B* **4**, 3533(1992).
- ¹¹D. Winske and K. B. Quest, *J. Geophys. Res.* **93**, 9681 (1988).
- ¹²R. E. Lowe and D. Burgess, *Ann. Geophys.* **21**, 671 (2003).
- ¹³E. L. M. Hanson, O. V. Agapitov, F. S. Mozer, V. Krasnoselskikh, S. D. Bale, L. Avakov, Y. Khotyaintsev, and B. Giles *Geophys. Res. Lett.* **46**, 2381 (2019).
- ¹⁴I. J. Cohen, S. J. Schwartz, K. A. Goodrich, N. Ahmadi, R. E. Ergun, S. A. Fuselier, M. I. Desai, E. R. Christian, D. J. McComas, G. P. Zank, et al., *J. Geophys. Res.* **124**, 3961 (2019).
- ¹⁵T. Umeda, M. Yamao, and R. Yamazaki, *Astrophys. J.* **695**, 574 (2009).
- ¹⁶M. Gedalin, *J. Geophys. Res.* **101**, 15569 (1996).
- ¹⁷M. Gedalin, *Geophys. Res. Lett.* **24**, 2511 (1997).
- ¹⁸M. Gedalin, *J. Plasma Phys.* **81**, 905810603 (2015).
- ¹⁹M. Gedalin, *Phys. Plasmas.* **22**, 072301 (2015).
- ²⁰L. Ofman, M. Balikhin, C. T. Russell, and M. Gedalin, *J. Geophys. Res.* **114**, A09106 (2009).
- ²¹L. Ofman and M. Gedalin, *J. Geophys. Res.* **118**, 1828 (2013).
- ²²T. Umeda, Y. Omura, T. Tominaga, and H. Matsumoto, *Comput. Phys. Commun.* **156**, 73 (2003).
- ²³T. Umeda and R. Yamazaki, Particle simulation of a perpendicular collisionless shock: A shock-rest-frame model, *Earth Planets Space* **58**, e41 (2006).
- ²⁴T. Umeda, M. Yamao, and R. Yamazaki, *Astrophys. J.* **681**, L85 (2008).
- ²⁵T. Umeda, Y. Omura, and H. Matsumoto, *Comput. Phys. Commun.* **137**, 286 (2001).
- ²⁶P. D. Hudson, *Planet. Space Sci.* **18**, 1611 (1970).
- ²⁷T. Umeda, Y. Kidani, S. Matsukiyo, and R. Yamazaki, *Phys. Plasmas* **19**, 042109 (2012).

²⁸T. Umeda, Y. Kidani, S. Matsukiyo, and R. Yamazaki, *Phys. Plasmas* **21**, 022102 (2014).

²⁹T. Hada, M. Oonishi, B. Lembège, and P. Savoini, *J. Geophys. Res.* **108**, 1233 (2003).

TABLE I. Upstream parameters and simulation results.

Run	Upstream parameters				Results			
	u_{x1}/v_{te1}	$\omega_{pe1}/\omega_{ce1}$	β_1	u_{x1}/V_{A1}	M_A	M_A^2/β_1	$\langle T_{i\perp}^{\max} \rangle / T_{i1}$	$T_{i\perp}^{\max} / T_{i1}$
A	1.875	2	0.08	6	5.2	334	183	160–205
B	0.9375	4	0.32	6	6.5	132	63.9	53.9–75.4
C	0.46875	8	1.28	6	6.1	28.6	14.9	13.4–17.1
D	1.25	2	0.08	4	4.6	265	101	86.5–123
E	0.625	4	0.32	4	4.7	70.5	30.0	26.2–35.5
F	0.3125	8	1.28	4	3.9	12.5	5.01	4.80–5.20

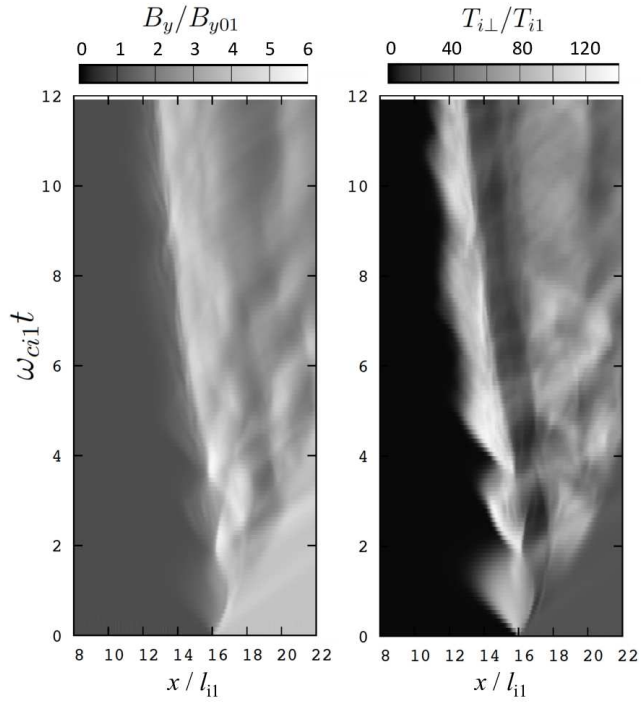


FIG. 1. Spatiotemporal diagram of the y -component of the magnetic field B_y and ion perpendicular temperature $T_{i\perp}$ for Run D. Both B_y and $T_{i\perp}$ are averaged over y direction. Initial unphysical discontinuity is located at $x = 16l_{i1}$.

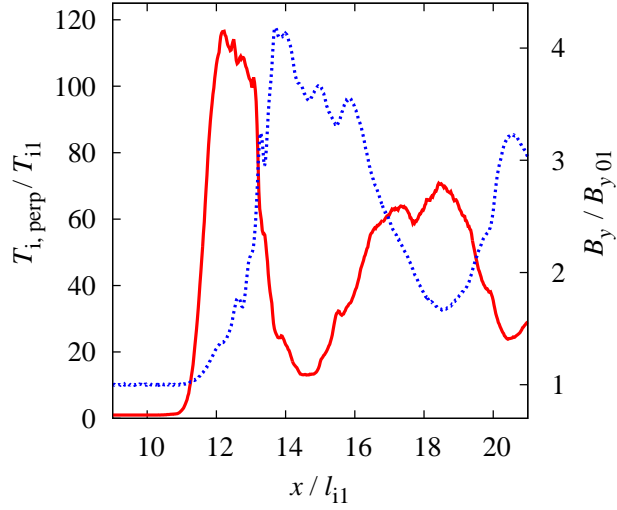


FIG. 2. Spatial profile of ion perpendicular temperature averaged over y direction, $T_{i\perp}$ (thick solid curve) and the y -component of the magnetic field averaged over y direction, B_y (dotted curve) at $\omega_{ci1}t = 9.96$ of Run D.

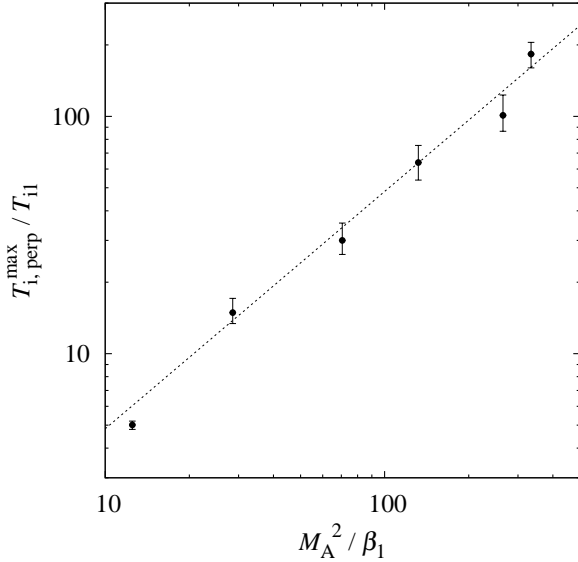


FIG. 3. Ion perpendicular temperature $T_{i\perp}^{\text{max}}$ as a function of M_A^2/β_1 . Triangles represent $\langle T_{i\perp}^{\text{max}} \rangle / T_{i1}$, while error bars indicate the maximum and minimum values of $T_{i\perp}^{\text{max}}/T_{i1}$, which are given in TABLE I. All the values are obtained for $7 < \omega_{ci1}t < 12$. Dotted line represents best-fitted linear relation, $T_{i\perp}^{\text{max}}/T_{i1} = 0.48 \times M_A^2/\beta_1$.